Morphology And Molecules: An Integrated Comparison Of Phenotypic And Genetic Rates Of Evolution

By: **Steven J. Hageman**

Abstract

The ability to successfully apply species and species concepts to real world problems such as biostratigraphy and conservation biology makes a strong argument for the existence of species (i.e., a level of organization that exists in the phenotype and genotype), whether or not we fully understand the processes involved in their origin. What we do know about the origin of biological species is drawn from four general perspectives: (1) Biological: variation within and among the broader phenotypes of closely related living organisms (including behavior, skeletal and nonskeletal morphology, physiology, and biochemistry, all generally limited to ecological timescales) and cross breeding hybridization experiments; (2) Molecular: genetic data consisting of coded nucleotide sequences (DNA) ranging from short spans of a few dozen base pairs of uncertain placement or function to well documented genes to entire genomes; (3) Paleontological: documentation of patterns and rates of morphologic change in closely related lineages through geologic time (primarily skeletal phenotypes); and (4) Theoretical considerations: some informed by the other three areas and others pure and independent.

Hageman, S.J. (2016). Morphology and Molecules: An Integrated Comparison of Phenotypic and Genetic Rates of Evolution, in *Species and Speciation in the Fossil Record* (pages 168-197), Eds. Warren D. Allmon & Margaret M. Yacobucci. Chicago : University of Chicago Press. 2016. ISBN 9780226377445.

Morphology and Molecules: An Integrated Comparison of Phenotypic and Genetic Rates of Evolution

Steven J. Hageman

Introduction

The ability to successfully apply species and species concepts to real world problems such as biostratigraphy and conservation biology makes a strong argument for the existence of species (i.e., a level of organization that exists in the phenotype and genotype), whether or not we fully understand the processes involved in their origin. What we do know about the origin of biological species is drawn from four general perspectives: (1) Biological: variation within and among the broader phenotypes of closely related living organisms (including behavior, skeletal and nonskeletal morphology, physiology, and biochemistry, all generally limited to ecological timescales) and cross-breeding hybridization experiments; (2) Molecular: genetic data consisting of coded nucleotide sequences (DNA) ranging from short spans of a few dozen base pairs of uncertain placement or function to well-documented genes to entire genomes; (3) Paleontological: documentation of patterns and rates of morphologic change in closely related lineages through geologic time (primarily skeletal phenotypes); and (4) Theoretical considerations: some informed by the other three areas and others pure and independent.

In the past 150 years, an enormous amount of data has been generated from these four perspectives toward understanding the processes and mechanisms of speciation. These include: (1) hundreds of empirical studies of rates of morphologic change (e.g., Cheetham, 1986; Lazarus, 1986; Stanley

and Yang, 1987; Geary, 1990; Budd and Klaus, 2008; Groves and Reisdorph, 2009; Pachut and Anstey 2009; Geary et al., 2010; Miller, chapter 2, this volume); (2) thousands of empirical studies of speciation in modern organisms based on variation of the phenotype (e.g., Belk, 1989; McPeek et al., 2010; Oros et al., 2010; Arkhipkina et al., 2012); and (3) mo lecular (genetic) data, requiring the organized efforts of federal governments and their consortia to house and store our current data set (e.g., National Center for Biotechnology Information, US National Institutes of Health). Finally, numerous theoretical ideas (e.g., Allmon and Ross, 1990; Levinton, 2001; Roopnarine, 2003; Coyne and Orr, 2004; Estes and Arnolod, 2007; Gingerich, 1983, 2009; Hunt, 2010; Allmon, chapter 3, this volume; Miller, chapter 2, this volume) have been proposed to interpret and explain these data.

Because of these efforts we do understand a great deal about how evolution works and the resulting diversity of life. However, I would argue that in the grand scheme, a gaping hole still exists in the middle ground between these perspectives that is Darwin's original curiosity: "The origin of species." How do the genes, combined with the whole phenotype and its environment, shift within populations to generate a new species, which in many cases can be identified by a portion of its phenotype (e.g., skeleton) and act in ways that appear to be disconnected across different scales of time?

Attempts at integrating phenotypic data with genetic data have largely concentrated on using data sets that combine molecular and morphologic data in a single cladistics analysis (e.g., Mishler, 1994; Giribet et al., 2000) or superimposing the results of independent molecular phylogenies with stratophenetic character states (e.g., Lydeard et al., 1995; Wahlberg and Nylin, 2003; Decellea et al., 2012; Jagadeeshan and O'Dea, 2012). Typically, these studies and have concentrated on rates of cladogenesis rather than documenting change within clades (Nee, 2004; Quental and Marshall, 2010).

The goal of this project is to integrate morphologic (skeletal phenotype) and molecular (genetic) data into a single analysis and to provide a model that can eventually be extended to methods that estimate rates of genotypic change within and among species-level clades based on calibrated rates of change through fossil phenotypes.

General Properties of an Integrated Model

A key to moving forward with our understanding of the process of speciation will be to study extant taxa that have an excellent fossil record, that is,

to simultaneously perform molecular and morphologic studies on a single suite of modern individuals and then trace their lineage through geologic time using both molecular phylogenies and stratophenetics.

Two simple models for morphologic change (fig. 5.1.1) and molecular change (fig. 5.1.2) through geologic time can be scaled and integrated into a single model (figs. 5.1.3 and 5.2.2). Figure 5.1.1 depicts a hypothetical situation of complete morphologic stasis for two closely related species A and B. The y-axis represents geologic time, a numerical chronology beginning with the present at the top (0.0 years), developed from all available and relevant sources (e.g., biostratigraphy, radiometric dating, chemostratigraphy). The x-axis represents any morphologic feature that can be adequately preserved in the fossil record so as to be quantified and compared among specimens. In this model, morphology could represent a simple linear measurement such as "length of nose," or a value derived from the ordination of a multivariate suite of characteristics such as a principal component score for observations from dozens of features for a specimen (e.g., Budd and Pandolfi, chapter 7, this volume), or any of the metrics resulting from morphometric methods that represent relationships among landmarks or describe shapes of organisms or their parts.

Figure 5.1.2 is a model of molecular change for a gene segment used in phylogenetic analysis, e.g., COI or 16s mRNA) versus time based on an empirical mutation rate (Freeland, 2006) for two extant sister species. The molecular distance (thick line A_0B_0) represents the percentage of nucleotide base pairs in common for the gene.

The molecular distance (genetic difference) between any two organisms, whether of the same population or even different phyla, will reflect the relative amount of time since the two had a common ancestor (Freeland, 2006; Beebee and Rowe, 2008). Beginning at the time that these two taxa shared a common ancestor (X in fig. 5.1.2), they will accumulate random mutations at a relatively constant rate; thus, the amount accumulated by either one is one-half the total distance (AY and BY, fig. 5.1.2). The mutation rate can be calibrated, especially for more closely related groups, using well-constrained divergence times based on fossils (Donoghue and Benton, 2007). Virtually any sequence or combination of partial sequences can be used to define the molecular distance between taxa, so long as the sequence is directly comparable among the taxa involved (Freeland, 2006; Beebee and Rowe, 2008).

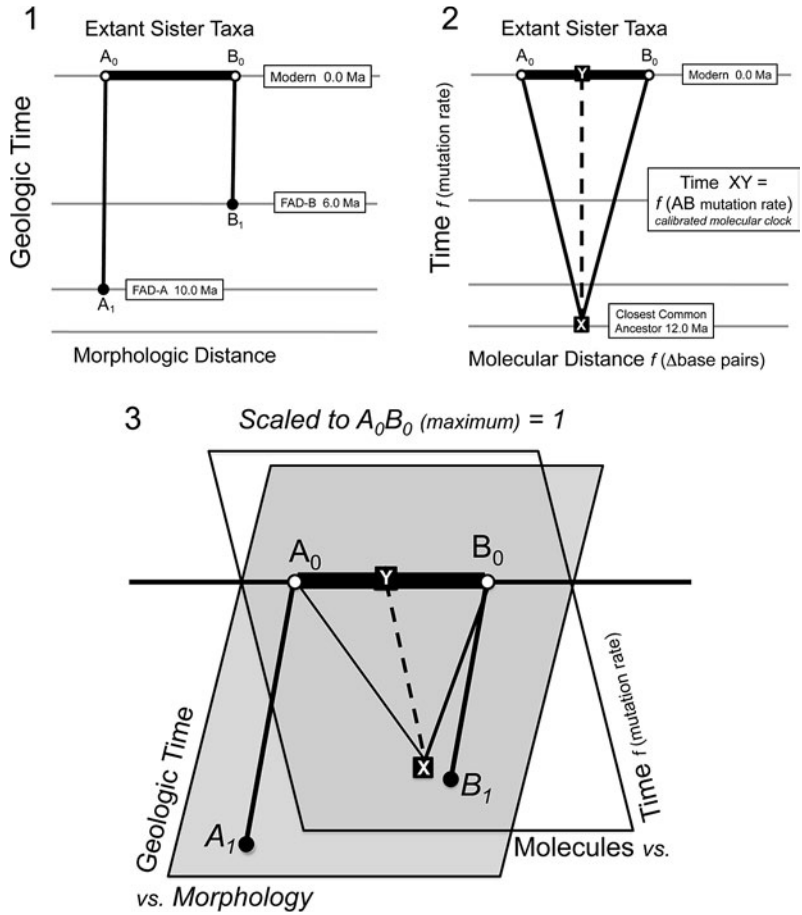

Figure 5.1 (1) Morphologic variation (phenotypic) versus geologic time, showing complete morphologic stasis of two sister species.
The morphologic distance (thick line A_0B_0) is constant through time and the first appearance datum for species A is 10.0 Ma (specimen A_1) and 6.0 Ma for species B (specimen B_1). Specimen A_0 is same species as A_1, the subscripts indicate position in time. (2) Molecular change (genetic) versus time as a function of mutation rate, showing gradual divergence at a constant rate for two sister species A and B. The molecular distance (thick line A_0B_0) increases through time (0 at inferred time of last shared ancestor "X" 12.0 Ma. Specimens A_0 and B_0 are the same individuals as those characterized morphologically in 5.1.1. (3) Mathematical spaces 1 and 2 overlap when specimens A_0 and B_0 are scaled to the same metric (maximum distance = 1.0), i.e., same two specimens for species A and B in each mathematical space.

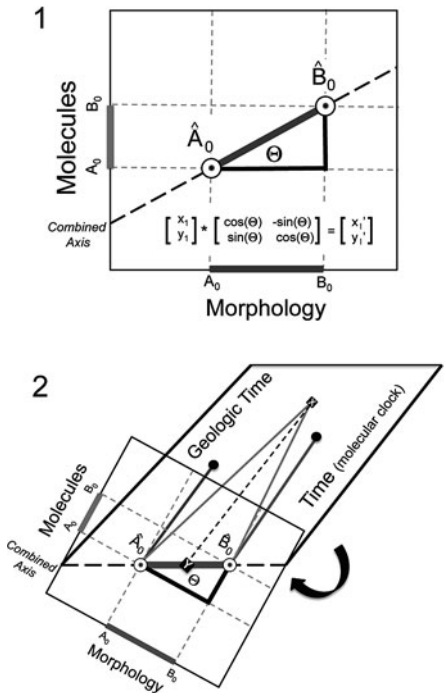

Figure 5.2 Model for an integrated analysis of morphology and molecules.
(1) Model for an integrated analysis of morphology and molecules. Each axis is scaled to the maximum value observed in the study (or another defined standard). A new, combined axis can be generated by rotating observations through the angle theta, where θ = arcsine of (Δ molecules/Δ morphology). These axes can be scaled because the line A_0B_0 for morphology is measured on the same specimens as the line A_0B_0 for molecules, thus the line between $\hat{A}_0$ and $\hat{B}_0$ is derived from the same specimens for both axes. (2) Because the combined axis for $\hat{A}_0$ and $\hat{B}_0$ represents both morphology and molecules (scaled), the geologic time axis of fig. 5.1.1 can be equilibrated with the molecular clock time axis of fig. 5.1.2. The result is an integrated model of morphology, molecules, and time (morpho-molecular-temporal space).

Derivation of an Integrated Model

Comparing figures 5.1.1 and 5.1.2, we can see that distance A_0B_0 for morphology and distance A_0B_0 for molecules are intimately related in that they are calculated on the exact same two specimens representing two different species. Thus scaled values for morphology and molecules A_0B_0 can be superimposed as an intersection of the two mathematical spaces (fig. 5.1.3). Values for morphologic A_0B_0 and molecular A_0B_0 can be represented

for the two specimens on a scatter plot (fig. 5.2.1). These two dimensions (morphology and molecules) can be scaled to unity, such that morphologic $A_0B_0 = 1.0$, molecular $A_0B_0 = 1.0$, and the integrated distance $\hat{A}_0$ and $\hat{B}_0$ can be calculated.

When only two specimens are used in the analysis the distance $\hat{A}_0$ to $\hat{B}_0$ will equal $\sqrt{2}$ and the angle theta (θ) will equal 45° (x and y each scaled to 1.0). However, when multiple specimens are employed in an analysis, if x is scaled to 1.0 = maximum morphologic distance and y is scaled to 1.0 = maximum molecular distance (not required to be from the same specimen pair), then all other pairwise comparisons of integrated data for specimens $\hat{A}_0$ to $\hat{B}_0$ can be compared to this standardized distance based on maximum A_0B_0 for morphology and molecules of the group of specimens under consideration. In practice, A_0B_0 of morphology and molecules can be scaled to any defined standard.

Once a new combined axis is created for morphology and molecules scaled to unity, the third dimension (time) can be projected behind the plane (fig. 5.2.2), which represents both morphology vs. geologic time (fig. 5.1.1) and molecules vs. calibrated molecular clock time (fig. 5.1.2). Because points $\hat{A}_0$ and $\hat{B}_0$ are identical (i.e., exact same specimens), we have a reference point on which all planes can be tied (5.1.3) allowing for the integrated model of figure 5.2.2, which can viewed from any perspective of the three dimensions (morpho-molecular-temporal space).

A limiting requirement of the methodology proposed here is that direct comparisons of taxa can only be made within a unique set of morphologic and molecular variables, i.e., modification of the list of characters, either morphologic or molecular, results in a new mathematical space that is not directly comparable to others. Therefore, selection of morphologic features (Ciampaglio et al., 2001) and molecular data (Freeland, 2006; Beebee and Rowe, 2008) should be given careful consideration at the outset, so as to maximize the utility of a given study.

Interpretation of Integrated Data

On the plane of scaled morphology and molecules (fig. 5.3), the maximum (100%) is defined by the maximum value of the absolute difference in the suite of specimens under study. For example, in figure 5.3, if the maximum difference between any pairwise comparison of taxa for the character "nose-length" was 2.0 cm, the morphologic axis would range from 0% = 0.0 cm

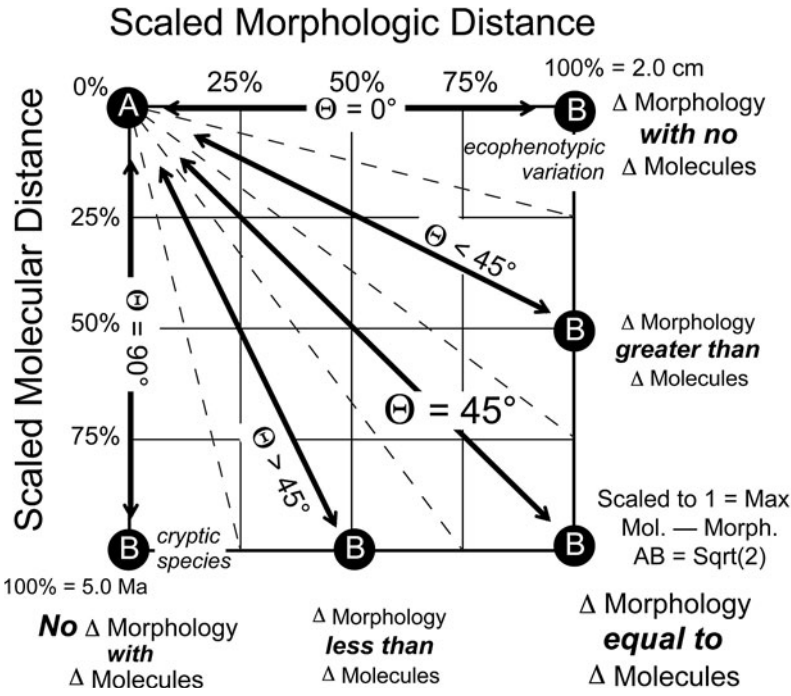

Figure 5.3 Model showing the relationship of angle theta (fig. 5.2.1) to relative rates of change in morphology and molecules in a system scaled by the maximum observed value on each axis.

Molecular distance of 0 = no divergence time between specimens = same population. Morphologic distance of 0 = no phenotypic variation between specimens, based only on the characteristics used in the analysis.

to 100% = 2.0 cm. The units of the scaled molecular distance will be based on the method used and number of nucleotide base pairs involved. This value (index of shared molecular code) can, however, be converted to a time interval using a calibrated molecular clock. Thus, for a study where the maximum difference in number of shared nucleotide base pairs at corresponding sites results in a maximum calculated molecular clock age of 5.0 Ma, the scaled molecular axis would range from 0% = 0.0 years (present day) to 100% = 5.0 Ma.

Scaling is a function of the angle theta (θ) through which each axis must be rotated in order to create a new combined axis through the two points (equation in fig. 5.2.1). Theta (θ) = arctangent of (Molecular A_0B_0 ÷ Morphologic A_0B_0). On plots of morphology vs. molecules, the angle theta

(θ from the rotational angle in fig. 5.2.1) will be 45° if there is a 1:1 relationship (fig. 5.3). All distances between pairwise specimen comparisons are scaled to this standard, the maximum observed morphologic and molecular distances (potentially from two different specimen pairs). The ratio of morphologic change to molecular change will be greater than, less than, or equal to the standard of maximum observed ($\hat{A}_0$ to $\hat{B}_0$ = 1.0 and θ = 45°).

Theta will *decrease* as the magnitude of molecular variation decreases relative to morphologic variation to the point where θ = 0° with no difference in molecules (all morphologic variation is environmentally controlled = ecophenotypic (i.e., no time for any accumulated molecular differentiation = same population, fig. 5.3). Theta will *increase* as the magnitude of molecular variation increases relative to morphologic variation to the point where θ = 90° with no difference in morphology (morphologically cryptic species, fig. 5.3).

Comparing differential rates of change using integrated data

Several hypothetical scenarios are presented in figure 5.4 in order to demonstrate how patterns can be interpreted. The mathematical space is defined on ten hypothetical species (A, B, C, D, F, G, H, X, Y, Z) and data are scaled to 100% morphologic change = 2.0 cm (A–G) and 100% molecular change = 5.0 Ma (A–Z). All distances in are plotted relative to species A (fig. 5.4), though each pairwise distance could be plotted in this space.

In figure 5.4.1, species F, G, and H have diverged from species A at rates where morphologic change exceeds molecular change (for variables that define this space). Species F and G have evolved for the same amount of time from species A (scaled molecular distance = 25% = 1.25 Ma for both), but species G has shown a greater amount of morphologic change. In comparison, species F and H show the same degree of morphologic change relative to species A (scaled morphologic distance = 75% = 1.50 cm of net change), but species H has diverged from A for twice as much time as F has from A (25% vs. 50% = 1.25 Ma vs. 2.50 Ma).

Figure 5.4.2 provides a scenario where four species (A, B, C, D) belong to one putative genus (lightly shaded circles) and three species (X, Y, Z) belong to a second putative genus (darkly shaded circles). This example shows that species B, C, and D have evolved at the same rate (θ < 45°, morphologic change faster than molecular change) and that their times since divergence from species A can be ordered (B, D, C). Species X,

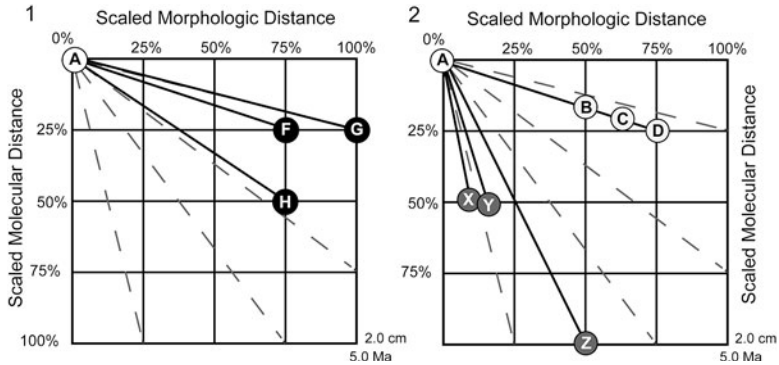

Figure 5.4 Hypothetical examples of different rates of morphologic and molecular evolution, relative to the standardized distance (maximum Δ morphology = AC = 1.0; maximum Δ molecules = AZ = 1.0).
(1) Three species (F, G, H), each compared to species A. Species F and G diverged from species A at the same time (25% of 5.0 Ma = 1.25 Ma), but species G had a greater amount of morphologic change than species F (100% vs. 75% of 2.0 = 2.0 cm and 1.5m cm change). In comparison, species H and F had equal morphologic change from species A (75% of 2.0 = 1.5 cm), but species H diverged from species A twice as long ago as species F did from A (50% vs. 25% of 5.0 Ma, 2.5 Ma and 1.25 Ma). (2. Three species of the same genus (B, C, D) showing successive divergence times from species A, but all at the same rate (morphology more rapid than molecules as compared to the standard). Two species of a different genus, species X and Y, diverged from species A at about the same time, with comparable rates of change (molecules changing faster than morphology relative to standard). Species Z is an outlier, inviting further investigation of its relationships to both species X and Y and it relative position to species A.

Y, and Z show faster relative molecular change ($\theta > 45°$). Species X and Y diverged from species A twice as long ago as did species B from A (50% = 2.50 Ma vs. 25% = 1.25 Ma). Species Z diverged from species A over three times as long ago as species B and its morphology has changed more rapidly than X and Y relative to the degree of its molecular change (fig. 5.4.2).

Evaluating hypothetical timing of first occurrence and common ancestors

By plotting expected molecular distance through geologic time using a calibrated molecular clock, scaled to the best chronologic data available for stratophenetics, one of three results could be expected (fig. 5.5).

If one species is a true sister taxon of the other (e.g., species B is a direct descendant of species A, fig. 5.5.1), the molecular estimate of the closest common ancestor X should be coincident with the first appearance of the

descendant species. The reason that these dates might not align exactly, even when the phylogenetic assumption is correct, include inaccuracies/imprecision in molecular clock calibration and or in chronostratigraphic resolution. Also, lack of alignment can occur when the first appearance datum does not adequately reflect the true origin of the species due to preservation or sampling bias. Statistical methods related to maximum likelihoods (i.e., error bars) can most likely be developed in order to determine the degree to which disagreement of molecular clock and chronostratigraphic dates are acceptable.

If the two taxa are not true sister species, but are part of a relatively close clade originating from other species not included in the plot, the calibrated molecular date will be older than the stratophenetic date of either. That is, figure 5.5.2 shows that based on molecular distance, species B shared a common ancestor with species A much earlier than the first occurrence of species B. Again, methods to determine whether this can be accounted for by an incomplete fossil record of species B, or inaccuracies of dating with molecular clock/chronostratigraphy, will have to be developed. But plots such as this can direct those inquiries.

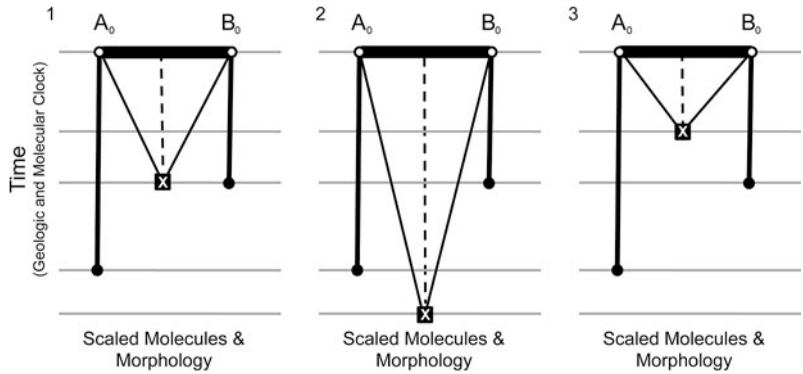

Figure 5.5 Models for three possible outcomes of comparing predicted times of youngest common ancestor for species pairs (assuming valid calibrated molecular clock and chronostratigraphy).
(1) Predicted time from molecules matches observed first appearance (or predicted time of origin), i.e., one could likely be the direct descendent of the other. (2) Predicted time from molecules significantly exceeds the observed first appearance (or predicted time of origin), which would indicate that either the observed stratigraphic ranges do not adequately represent the true ranges of the taxa, or both taxa share third, unidentified, common ancestor. (3) Predicted time from molecules is significantly less than the observed first appearance (or predicted time of origin), which suggests that error exists in identification of some specimens within the study.

In a similar scenario, if the timing of a closest common ancestor is significantly younger than the first occurrence of either taxa (fig. 5.5.3), this should raise questions about the validity of the assumption that these are true sister species (again accounting for acceptable variation due to molecular and chronostratigraphic dating).

Selection of Molecules, Morphology, and Distance Metrics

Molecular characters

Very few genes have been tied directly to morphologic variation in the phenotype (Gompel et al., 2005). Genes and partial gene sequences are used in most phylogenetic applications, e.g., COI cytochrome oxidase is mitochondrial and codes for proteins with physiological functions (Freeland, 2006; Beebee and Rowe, 2008); 12s rRNA and 16s rRNA are also mitochondrial (plus prokaryotes) and code for parts of the ribosome. Commonly used nuclear genes (18S, 28S) also code for ribosomes (Freeland, 2006; Beebee and Rowe, 2008). In fact, many phylogenetic applications use noncoding parts of the genome such as internal transcribed spacer (ITS) between regions that code for ribosomes (Freeland, 2006; Beebee and Rowe, 2008). These random, nonfunctioning mutations collect in the ITS regions.

Thus, the molecules used in this and in most studies of evolution serve as accumulated mutations (molecular clocks originally proposed by Zuckerkandl and Pauling [1962, 1965]) or proxies for relative amount of time since two taxa shared a common ancestor. Molecular clocks can be calibrated using geochronologically established divergence times from the fossil record (Omland, 1997; Donoghue and Benton, 2007). Because rates of molecular change are not fixed absolutely even within clades (Ayala, 1997; Drummond et al., 2006), molecular clocks can be modeled as relaxed or variable across branches (Drummond et al., 2012; Jagadeeshan and O'Dea, 2012).

In addition to options for selecting a molecular distance metric, there are also several strategies for calibrating molecular clocks (Sanderson, 2002; Kumar, 2005; Dornburg et al., 2011), but similar to complexities with morphologic change through time (fig. 5.6), any of these could be incorporated into a more complex model than the one proposed here.

In a most simple calculation of molecular distance, two taxa may be compared based on how many nucleotide base pairs (bp) they share, e.g.,

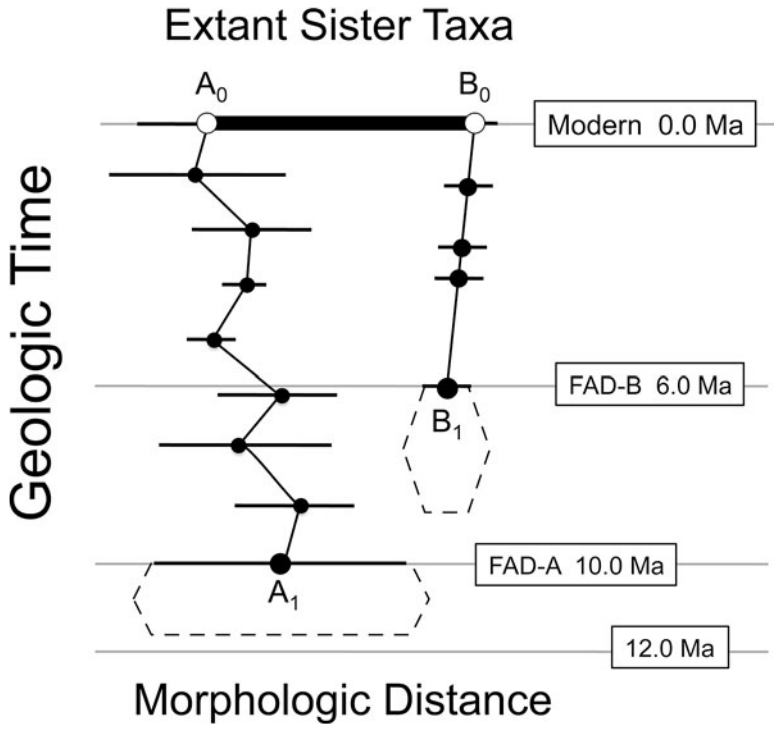

Figure 5.6 A hypothetical model of morphologic variation (phenotype) versus geologic time. This model, which is more complex and realistic than fig. 5.1.1, shows both anagenesis in mean morphology for species B and reversals (zigzags) of mean phenotypes for species A. The amount of variation within samples (horizontal lines) is great for species A, but nearly constant for species B. The morphologic distance (thick line A_0B_0) is variable through time. The actual time and morphology at the origin of each species is approximated within the dashed borders.

two taxa sharing 95% of 650 bp would be much closer in molecular space than two taxa sharing 87% of the same sequence.

The method typically used to calculate uncorrected nucleotide distance between any two taxa (*p-distance*) (Nei and Kumar, 2000; Yang, 2006) is expressed as

$$\hat{p} = n_d/n, \text{where}$$

n_d = number of bp sites with different nucleotides between the two sequences, and

n = total number of nucleotide bp sites examined.

The variance of $\hat{p}$ (Nei and Kumar 2000; Yang, 2006) is

$$V(\hat{p}) = p(1-p)/n.$$

P-distance is usually an adequate index for closely related taxonomic comparisons, but it does not account for backwards or parallel substitutions (Yang, 2006) nor complexities that arise because of different processes of mutation (Nei and Kumar, 2000), i.e., substitution (exchange at one site), deletion (everything shifts), or inversion (two ends pivot around middle third) (Nei and Kumar, 2000). In addition, some of these processes operate with different likelihoods depending on the nucleotides involved, e.g., (T or C) vs. (A or G) (Nei and Kumar, 2000).

For large p (molecular distances), more complex models are required based on probabilities of nucleotide pairs, e.g., Kimura's Two-Parameter Method or Tamura and Nei's Method (Nei and Kumar, 2000). For this study, the Kimura 2-parameter model (K2P of Kimura, 1980) with a discrete approximation of the Γ distribution (K2P + Γ) was used to calculate molecular distance (data from Dick et al., 2003). This results in a p-distance expressed in units of percent difference (Nei and Kumar, 2000).

Morphologic characters

Virtually any kind of morphologic data can be used so long as they can be defined, collected, and treated uniformly across all specimens for study. Although the morphologic portion of the space will have greatest relevance when constructed as part of a hypothesis based in paleobiological theory, the methodology does not require this.

A suite of closely related specimens should be incorporated into a model (not just a single pair). Subsets of the total can be plotted individually, but once the space is defined by a set of specimens, morphologic characters and molecular description of a new model must be generated if any specimens are added.

Figure 5.6 represents some of the complexities of morphologic change and properties of empirically collected data. These complexities are intentionally omitted from the development of a model that integrates morphology and molecules; however, many of these issues have been studied in detail and in many cases practical solutions have been proposed that can be included directly into a more comprehensive integrated model. Complexities present in figure 5.6 include:

1. Patterns of change within species through time from stasis to anagenesis, random walk, or a combination (Bookstein, 1987; Gingerich, 1983, 2009; Cheetham and Jackson, 1995; Roopnarine et al., 1999; Hunt, 2010, 2012).

2. Variation within samples (range, confidence intervals, relative analysis of average only) (e.g., Hageman, 1994; Renaud et al., 2007; Pachut and Anstey, 2009), and changes in variance among samples through time, i.e., variable width of sample error bars (e.g., Hageman, 1994; Ricklefs, 2006).

3. Temporal resolution and correlation of samples (e.g., Sadler, 1981, 2004; Kidwell and Bosence, 1991; Kowalewski and Bambach, 2008).

4. Uncertainty of first occurrence vs. evolutionary origin of a taxon (Marshall, 1990, 1997; Weiss and Marshall, 1999; Hayek and Bura, 2001).

5. Amount of morphologic variation that is due to environmental effects rather than genetic control, i.e., estimating the partitioning of the amount of the total variance that is caused by heritable genetic factors vs. environmental/other factors (Falconer, 1981; Jackson and Cheetham, 1990; Cheetham et al., 1993, 1994; Hunter and Hughes, 1994; Riisgård and Goldson, 1997; Hageman et al., 1999, 2009, 2011).

Case Study of Integrated Molecular and Morphologic Data

In a series of three papers (Dick et al., 2003; Herrera-Cubilla et al., 2006, 2008), a research group analyzed molecular and morphologic data for the same suite of specimens assigned to nine species in two genera (*Cupuladria* and *Discoporella*) from a single family (Cupuladridae) of modern bryozoans. These data are well suited to demonstrating the integrated methodology proposed here. Jagadeeshan and O'Dea (2012) recently published a study using the same kinds of morphologic and molecular data, which refine some of the species-level taxonomy for Panamanian Cupuladridae. The nomenclature of Dick et al. (2003) and Herrera-Cubilla et al. (2006 and 2008) is used here because it applies to the particular specimens employed in this study. The data set and methods of Jagadeeshan and O'Dea (2012) are also very well suited to the methodology proposed here.

Although change associated with a single morphological character may be interpreted more intuitively, Cheetham (1987) cautioned against interpreting patterns of evolution based on single morphologic features. Suites of related characters can carry more paleobiological significance. Regardless of how many characters are incorporated into a single analysis, the selection of characters to represent the morphologic phenotype should be

1

Loading Coefficients

	PCA-1	PCA-2	PCA3
Zl	0.141	**0.649**	-0.520
Zw	0.091	**0.594**	0.006
Ol	**0.937**	-0.268	-0.103
Ow	**0.257**	0.190	0.157
Al	0.159	0.301	**0.606**
Aw	0.056	0.165	**0.572**
variance	85.0%	13.2%	1.3%

2

Scores on Principal Component Axes

Species	PCA-1	PCA-2	PCA-3
C. biporosa	0.045	-0.012	0.002
C. exfragminis	0.046	-0.021	0.008
C. surinamensis	0.081	0.015	-0.008
D. bocasdeltoroensis	-0.033	-0.010	-0.008
D. terminata	-0.044	-0.024	-0.003
D. scutella	-0.021	0.027	0.003
D. cookae	-0.019	0.016	0.005
D. marcusorum	-0.027	0.004	0.001
D. marcusorum	-0.027	0.004	0.001

3

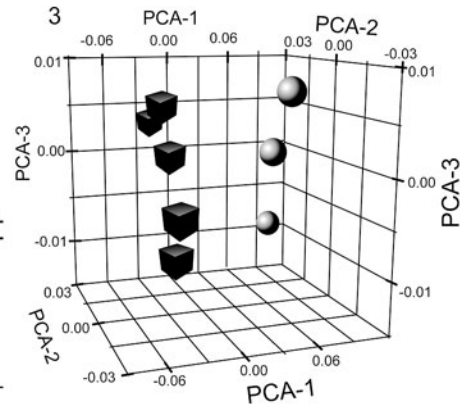

Figure 5.7 Principal component analysis of cupuladriid bryozoans (nine species, six characters). (1) Loading coefficients from principal components analysis of data from table 5.1, transformed (log10 (x+1)), with largest loadings in boldface. (2) PCA scores for each species on the first three axes. (3) Scatter plot of PCA scores. The loading coefficients for PCA-1 are dominated by opesia size, which differentiates between genera (spheres = *Cupuladria*, cubes = *Discoporella*). PCA-2 represents zooecia size and PCA-3 represents aperture size, both of which differentiate species within genera on the scatter plot. The first three axes account for 99.5% of total variance.

hypothesis driven. In order to identify a subset of characters with discriminatory power among cupuladriid species, data for over 25 characters available from Herrera-Cubilla et al. (2006, 2008) were analyzed using principal component analysis (PCA). A subset of six was chosen based on loading coefficients (fig. 5.7.1, table 5.1). These include the length and width of zooecia, opesia, and apertures (Zl, Zw, Ol, Ow, Al, Aw). These features are related to the shape and size of autozooecia (primary modules) in the bryozoan family Cupuladridae (characters defined and illustrated in Herrera-Cubilla et al., 2006, fig. 1.6, table 1).

Scores from PCA, nine species and six characters, were derived using PAST v. 2.15, with raw morphologic data (mm) transformed as log10 (1+ x) prior to PCA analysis. For these data (table 5.1, fig. 5.7), the variables Ol and Ow (opesia length and width) dominate the loading coefficients of PCA-1 (fig. 5.7.1), whereas PCA-2 and PCA-3 are dominated by zooecia (Zl, Zw) and aperture (Al, Aw) size. To demonstrate the methodology, I use the score for each species on PCA-1 (fig. 5.7.2). From a plot of PCA scores (fig. 5.3), we can expect PCA-1 to differentiate species between the two genera, whereas PCA-2 and PCA-3 differentiate species within genera. These insights may also guide the selection of characters used to define the morphospace for study.

TABLE 5.1. **Raw data for six morphologic characters from nine species of cupuladriid bryozoans, from Herrera-Cubilla et al. (2006, table 1) and Herrera-Cubilla et al. (2008, table 5), Z = zooecia, O = opesia, A = aperture, l = length and w = width, all measurements in mm.**

Species	abbreviation	Zl	Zw	Ol	Ow	Al	Aw
Cupuladria 4 (Cupuladria biporosa)	*Cbipor*	0.447	0.317	0.321	0.180	0.214	0.161
Cupuladria 5 (Cupuladria exfragminis)	*Cexfr*	0.423	0.294	0.330	0.181	0.218	0.173
Cupuladria 6 (Cupuladria surinamensis)	*Csuri*	0.547	0.371	0.406	0.219	0.235	0.165
Discoporella 2 (Discoporella bocasdeltoroensis)	*Dboca*	0.440	0.290	0.120	0.120	0.170	0.140
Discoporella 8 (Discoporella terminata)	*Dterm*	0.390	0.270	0.100	0.120	0.150	0.140
Discoporella 7 (Discoporella scutella)	*Dscut*	0.500	0.370	0.120	0.160	0.210	0.180
Discoporella 3A (Discoporella cookae)	*Dcook*	0.480	0.340	0.130	0.150	0.220	0.170
Discoporella 3B (Discoporella marcusorum)	*DmarB*	0.450	0.320	0.120	0.140	0.200	0.150
Discoporella 3C (Discoporella marcusorum)	*DmarC*	0.450	0.320	0.120	0.140	0.200	0.150

The following is an outline of the protocol that can be used to produce the integrated model for the example case. Begin with a matrix of morphologic distances between every taxonomic pair (upper-right of table 5.2.1) calculated as the absolute value of $(x_i - x_n)$ from morphologic data (here, PCA-1 scores, fig. 5.7.2). Then calculate each pairwise difference as a percentage of the maximum observed morphologic difference (upper-right of table 5.2.2), e.g., 0.036 / 0.125 * 100 = 28.8% (*C. biporosa* vs. *C. surinamensis*).

In a similar manner, use a pairwise matrix of molecular distances between every taxonomic pair (lower-left of table 5.2.1), here as absolute value (K2P + Γ) differences (from Dick et al., 2003, lower part of their table 3). Then calculate each pairwise difference as a percentage of the maximum observed molecular difference (lower-left of table 5.2.2), e.g., 17.27 / 25.8 * 100 = 66.9% (*C. biporosa* vs. *C. surinamensis*).

Then, create a new table where x = % morphologic distance (upper-right of table 5.2.2) and y = % molecular distance (lower-left of table 5.2.2). Resulting scatter plots (fig. 5.8) will have x-axis values from 0% = 0.000 to 100% = 0.125 scores on PCA-1, dominated by the size of the opesia. The resulting y-axis has values from 0% = 0.00 to 100% = 25.8 (K2P + Γ distance), which can be converted to 14.03 Ma using an estimated

TABLE 5.2. **(1) Similarity matrix for nine species assigned to two genera. Upper-right half of matrix is distances between paired taxa based on PCA-1 scores. The lower-left is molecular distances for 16s mRNA from Dick et al. (2003) for the same specimens. (2) Similarity matrix for the same specimens, expressed as a percentage of the maximum value observed in 1 (in bold). Percentages were used in scatter plots for fig. 5.9 (upper-right = morphology = x-axis; lower-left = molecules = y-axis).**

1

	Cupuladria 4 (C. biporosa)	*Cupuladria 5 (C. exfragminis)*	*Cupuladria 6 (C. surinamensis)*	*Discoporella 2 (D. bocasdeltoroensis)*	*Discoporella 8 (D. terminata)*	*Discoporella 7 (D. scutella)*	*Discoporella 3A (D. cookae)*	*Discoporella 3B (D. marcusorum)*	*Discoporella 3C (D. marcusorum)*
Cupuladria 4 (C. biporosa)	0.90	0.00	0.002	0.036	0.077	0.089	0.065	0.064	0.072	0.072
Cupuladria 5 (C. exfragminis)	5.7	0.46	0.00	0.034	0.079	0.090	0.067	0.066	0.074	0.074
Cupuladria 6 (C. surinamensis)	17.3	20.2	0.73	0.00	0.113	0.125	0.101	0.100	0.108	0.108
Discoporella 2 (D. bocasdeltoroensis)	25.0	25.8	19.5	0.14	0.00	0.011	0.012	0.013	0.005	0.005
Discoporella 8 (D. terminata)	20.5	23.8	15.7	13.6	0.14	0.00	0.023	0.025	0.017	0.017
Discoporella 7 (D. scutella)	22.7	24.3	18.3	16.9	13.3	0.18	0.00	0.001	0.007	0.007
Discoporella 3A (D. cookae)	22.9	25.4	19.1	17.2	12.3	7.5	0.37	0.00	0.008	0.008
Discoporella 3B (D. marcusorum)	22.8	24.9	19.8	19.3	13.6	8.9	3.2	0.26	0.00	0.000
Discoporella 3C (D. marcusorum)	22.7	24.8	20.4	19.2	15.8	10.0	4.2	4.5	1.15	0.00

16s Molecular (K2P + Γ) Distances (%)

Morphologic (PCA-Axis One) Distances

2

	Cupuladria 4 (C. biporosa)	*Cupuladria 5 (C. exfragminis)*	*Cupuladria 6 (C. surinamensis)*	*Discoporella 2 (D. bocasdeltoroensis)*	*Discoporella 8 (D. terminata)*	*Discoporella 7 (D. scutella)*	*Discoporella 3A (D. cookae)*	*Discoporella 3B (D. marcusorum)*	*Discoporella 3C (D. marcusorum)*	
Cupuladria 4 (C. biporosa)	3.3	0.00	1.3	28.8	62.1	71.2	52.5	51.3	57.8	57.8
Cupuladria 5 (C. exfragminis)	22.1	1.8	0.00	27.4	63.4	72.6	53.8	52.7	59.1	59.1
Cupuladria 6 (C. surinamensis)	66.9	78.4	2.8	0.00	90.9	100.0	81.3	80.1	86.6	86.6
Discoporella 2 (D. bocasdeltoroensis)	97.0	100.0	75.7	0.5	0.00	9.1	9.6	10.8	4.3	4.3
Discoporella 8 (D. terminata)	79.3	92.3	60.8	52.7	0.5	0.00	18.7	19.9	13.4	13.4
Discoporella 7 (D. scutella)	88.0	94.0	70.9	65.7	51.6	0.7	0.00	1.2	5.3	5.3
Discoporella 3A (D. cookae)	88.9	98.6	74.0	66.7	47.8	29.1	1.4	0.00	6.5	6.5
Discoporella 3B (D. marcusorum)	88.3	96.7	76.9	74.6	52.8	34.3	12.3	1.0	0.00	0.0
Discoporella 3C (D. marcusorum)	88.1	96.3	79.2	74.6	61.2	38.6	16.3	17.3	4.5	0.00

% of Maximum 16s Molecular (K2P + Γ) Distance

% of maximum Morphologic (PCA-Axis One) Distance

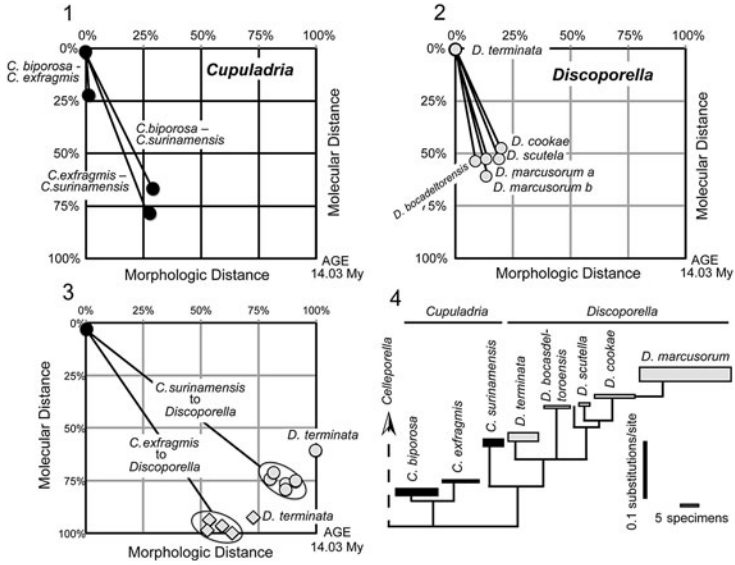

Figure 5.8 Single, scaled morpho-molecular space for nine cupuladriid species, with subsets of data plotted separately.
(1) Distances between paired species of the genus *Cupuladria* plotted in all combinations. *C. bipora* and *C. exfragmis* are the most closely related (diverged 22.1% of 14.03 Ma) and show very little morphologic change (1.3% of maximum PCA-1 difference for all nine species). *C. bipora* and *C. exfragmis* show about the same amount of morphologic divergence from *C. surinamensis,* but *C. exfragmis* apparently diverged earlier (78.4% of 14.03 Ma). (2) Distances between five species of the genus *Discoporella* each compared to *D. terminata*. See text for discussion. (3) Comparisons across genera. All *Discoporella* compared to *C. surinamensis* (maximum morphologic difference for PCA-1 scores) and *C. exfragmis* (maximum molecular difference). Species of *Discoporella* group in both comparisons, with the exception of *D. terminata*. (4) Phylogeny for the species represented, after Dick et al. (2003, fig. 4).

molecular clock for these specimens (25.8% bp difference maximum) ÷ (1.84% bp difference per million years mutation rate) based on the closing of the Isthmus of Panama (Dick et al., 2003).

A molecular phylogeny (16s) for the nine species from Dick et al. (2003, fig. 4) is summarized in fig. 5.8.4. Figure 5.8.1 shows the morphologic vs. molecular distance for the three species of the genus *Cupuladria* (scaled to maximum distances among all nine species). Results can be interpreted as follows. (1) Species pair *C. bipora* and *C. exfragmis* are nearly identical based on scores for PCA-1 (predominately opesia length and width) but have diverged in the 16s molecular composition over approximately 3.1 my (22.1% of 14.03 my). (2) Species *C. bipora* and *C. exfragmis* diverged

from *C. surinamensis* at 9.39 Ma and 11.00 Ma (66.9% and 78.4%) respectively, but the amount of morphologic divergence is about the same (28.5% and 27.4% of the total for PCA-1).

Figure 5.8.2 shows the scaled morphologic vs. molecular distance for five species of the genus *Discoporella* all from a sixth species, *D. terminata* (other pairwise species combinations are not illustrated). Results can be interpreted as follows. 1) All five species diverged from *D. terminata* during a relatively short interval (6.01–8.59 Ma), and species *D. bocadeltorensis* and *D. marcusorum* b, diverged from *D. terminata* within 7.40–7.41 Ma (Fig. 5.8.2). This close timing of divergence does not necessarily mean that these species are sister taxa, only that molecularly they are equidistant from *D. terminata*. These species have had comparable rates of morphologic change (13.4% to 19.9% of the total variation on PCA-1) (Fig. 5.8.2).

Figure 5.8.3 shows the scaled morphologic vs. molecular distance for each species of the genus *Discoporella* to the cupuladriid species with maximum morphologic difference (*C. surinamensis*) distances plotted with circles (fig. 5.8.3) and the species with greatest molecular difference (*C. exfragmis*) distances plotted with diamonds (fig. 5.8.3). Because these are not the same species in this case, no species plots 100% simultaneously for both axes. Results can be interpreted as follows. (1) In both cases, five of the *Discoporella* species plot in a cluster (ovals in fig. 5.8.3). The molecular distance values near 100% for *C. exfragmis* and most *Discoporella* species suggest a divergence time for these genera at 14.03 Ma. The suggested time of divergence based on *C. surinamensis* and most *Discoporella* species of about 10.6 Ma (75.4% of 14.03 Ma) is comparable to the estimated divergence time of these two cupuladriid species *C. exfragmis* and *C. surinamensis* 11.0 Ma (78% of 14.03 Ma). (2) In both sets of comparisons, *D. terminata* is an odd specimen out (fig. 5.8.3). It is unclear why it plots separate from other *Discoporella* species, but one of the roles of this methodology is to screen for outliers and investigate potential explanations.

Results for relative rates of morphologic and molecular change in these nine cupuladriid species (fig. 5.8) demonstrate the viability of the methodology and interpretation of empirical results. Clearly, the scale of the morpho-molecular space one defines will affect the relative distances among taxa. In this case, for instance, defining the space based only on *Discoporella* specimens (as compared to one defined by *Discoporella* and *Cupuladria* combined) may provide different insights.

Discussion: The Disconnect between Morphology and Molecules

When the model for complete morphologic stasis of species is integrated with the model for a molecular clock (fig. 5.9), the concerns expressed about processes to explain punctuated equilibrium (Eldredge and Gould, 1972; Gould and Eldredge, 1993; Ruse, 2000) are evident in the inescapable expectation that as molecular difference is traced back in time (diagonal lines in fig. 5.9), the distance between two related taxa by definition must be shorter and shorter.

This disconnect between rates of morphologic evolution and molecular evolution results in all forms of confounding observations including differing amounts of molecular distance between taxa through time that otherwise show constant morphologic distance (cf. fig. 5.9, species A and B at times T_2, T_1, and T_0). In cases where two species are not distinguishable based on the morphologic characters analyzed (or potentially any morphologic character), the morphologic lines of the species in a comparable figure 5.9 would be centered and indistinguishable, while the morphologic distance would inevitably diverge, resulting in cryptic species (Knowlton, 1993; Bickford et al., 2006).

The simple answer to this apparent paradox is that molecules used in molecular phylogenies are not the molecules that code for morphology (Pagel et al., 2006; Zeh et al., 2009; Rebollo et al., 2010). An entire field of biology—evo-devo, evolution and development—has developed in the past few decades that addresses questions about development and the specific genes that control the phenotype (Hageman, 2003; Carroll, 2005, 2007, 2009; Prud'homme, 2006, 2007).

In theory, relatively small mutations in a short region of DNA (regulatory elements) act on a conserved region of DNA (e.g., homeotic regulatory genes) that codes for body plans and morphology (Stone and Wray, 2001; Hoekstra and Coyne, 2007). Thus, the notion of "hopeful monsters," i.e., large shifts in morphology in single generation/mutation, is not that farfetched (Theissen, 2006; Rieseberg and Blackman, 2010). Theories from the field of evo-devo are intuitive and elegant in explaining observed paleontological patterns of macroevolution such as arthropod segment differentiation and specialization of appendages (Carroll et al., 2004; Carroll 2008, 2009) and the evolution of tetrapod limbs (Shubin, 2008). However, the genetic pathways through homeotic regulatory genes to specific phenotypes

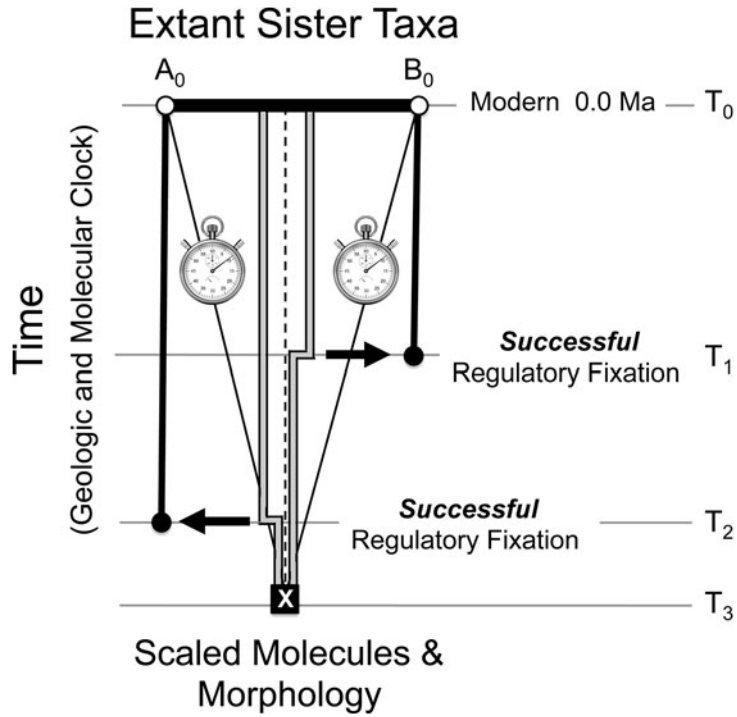

Figure 5.9 Integrated model of morphologic and molecular change through time. Line A_0B_0 represents scaled morphologic distance and molecular distance based on the maximum observed values in the suite of specimens being analyzed. Vertical axis represents geologic time calibrated to a molecular clock and chronostratigraphy. Straight vertical lines represent morphology of a species through time (complete stasis in this example). Diagonal lines represent molecular change (typical phylogenetic molecule), with the % base pair difference converging on zero at the time of the most recent common ancestor. Stepped thick lines represent base pair differences in regulatory elements that control the morphology in question. Accumulation of mutations in the molecules (thin diagonal lines) is steady and allows for a background clock. Accumulation of mutations in the regulatory elements (stepped thick lines) is irregular and can result in large, instant shifts in morphology.

can be identified only in model organisms thus far (Gompel et al., 2005; Davidson, 2010; Frankel et al., 2011; Wittkopp and Kalay, 2012).

Consider the model in figure 5.9. The diagonal lines represent the slow accumulation of mutations (all benign or entirely noncoding) in the genes typically used for phylogenetic analysis (e.g., COI or 16s). These accumulate at a relatively constant rate, as a predictable molecular clock (background stopwatch in fig. 5.9). The regulatory elements that are essential for coding morphology are represented by the thick gray lines in figure 5.9. Little is

known about the actual mutation rate of these and other genes related to morphogenesis. They could mutate at exactly the same rate as those genes used for phylogenetic analysis or they could be faster or slower, but there is no reason to expect them to not mutate at some average rate. The difference, however, is that mutation of a regulatory element or other key gene involved in morphogenesis has a greater likelihood of being lethal to the individual. It would only be the rare event of a nonlethal mutation that is favorably selected for, is fixed, and eventually enters the broader gene pool that will appear in the fossil record as a novel morphology. Depending on the magnitude of the morphologic change, this could appear as a punctuated event or a small directional shift (fig. 5.9). The thick gray lines in fig. 5.9 depict successful shifts (fixation) of a hypothetical regulatory element or gene essential to morphogenesis. All of the other random mutations in these genes would be culled under negative selection, i.e., regulatory elements do not accumulate benign or noncoding sequences as do most genes applied in phylogenetics. Through time, the accumulated genetic distance based on regulatory elements would be minor (fig. 5.9, thick gray lines) and would probably not accumulate at a constant rate (though they may be mutating at a predictable rate in the background). We do not yet have data to document the specific regulatory elements (genetic code) that could provide a mechanism for these shifts.

Even if a "regulatory element" explanation for morphologic microevolution and speciation proves misdirected, this should not inhibit paleontologists from documenting the patterns of morpho-molecular change within and among closely related species in anticipation of the inevitable recognition of the systems that do control morphogenesis and its evolution (Carroll, 2009; Davidson, 2010). As paleontologists, we can begin to document the connections and disconnections between molecules (phylogenetic) and morphology and use them to identify/predict potential mutation and fixation of whichever molecules are responsible for morphogenesis. This knowledge can provide constraints on a framework for interpreting patterns of microevolution throughout geologic time.

Acknowledgments

I thank W. D. Allmon and M. M. Yacobucci for organizing the topical session on fossil species at the Minneapolis GSA meeting 2011. I also thank M. M. Yacobucci, J. Pachut, and G. Hunt for careful review and suggestions that improved this paper.

References

Arkhipkina, A. I., A. B. Vyacheslav, and D. Fuchs. 2012. Vestigial phragmocone in the gladius points to a deepwater origin of squid (Mollusca: Cephalopoda). *Deep Sea Research Part I: Oceanographic Research Papers* 61:109–122. doi:10.1016/j.dsr.2011.11.010

Allmon, W. D., and R. M. Ross. 1990. Specifying causal factors in evolution: The paleontological contribution. In *Causes of Evolution: A Paleontological Perspective*, edited by R. M. Ross, and W. D. Allmon, 1–17. Chicago: University of Chicago Press.

Ayala, F. J. 1997. Vagaries of the molecular clock. *Proceedings of the National Academy of Science USA* 94:7776–7783.

Beebee, T., and G. Rowe. 2008. *An Introduction to Molecular Ecology*, 2nd ed. New York: Oxford University Press.

Belk, D. 1989. Identification of species in the conchostracan genus *Eulimnadia* by egg shell morphology. *Journal of Crustacean Biology* 9:115–125. doi:10.1163/193724089X00269

Bickford, D., D. J. Lohman, N. S. Sodhi, P. K. L. Ng, R. Meier, K. Winker, K. K. Ingram, and I. Das. 2006. Cryptic species as a window on diversity and conservation. *Trends in Ecology and Evolution* 22:148–155. doi:10.1016/j.tree.2006.11.004

Bookstein, F. L. 1987. Random walk and the existence of evolutionary rates. *Paleobiology* 13:446–464.

Budd, A. F., and J. S. Klaus. 2008. Early evolution of the *Montastraea* "*annularis*" species complex (Anthozoa: Scleractinia): Evidence from the Mio-Pliocene of the Dominican Republic. In *Evolutionary Stasis and Change in the Dominican Republic Neogene*. Topics in Geobiology, 30, edited by R. H. Nehm and A. F. Budd, 85–123. New York: Springer.

Carroll, S. B. 2005. *Endless Forms Most Beautiful: The New Science of Evo Devo and the Making of the Animal Kingdom*. New York: W. W. Norton & Company.

Carroll, S. B. 2007. *The Making of the Fittest: DNA and the Ultimate Forensic Record of Evolution*. New York: W. W. Norton & Company.

Carroll, S. B. 2008. Evo-devo and an expanding evolutionary synthesis: a genetic theory of morphological evolution. *Cell* 134:25–36. doi:10.1016/j.cell.2008.06.030

Carroll, S. B. 2009. *Remarkable Creatures: Epic Adventures in the Search for the Origin of Species*. Boston: Houghton Mifflin Harcourt.

Carroll, S. B., J. K. Grenier, and S. D. Weatherbee. 2004. *From DNA to Diversity: Molecular Genetics and the Evolution of Animal Design*, 2nd ed. Oxford: Wiley-Blackwell.

Cheetham, A. H. 1986. Tempo of evolution in a Neogene bryozoan: Rates of morphologic change within and across species boundaries. *Paleobiology* 12:190–202.

Cheetham, A. H. 1987. Tempo of evolution in a Neogene bryozoan: Are trends in single morphologic characters misleading? *Paleobiology* 13:286–296.

Cheetham, A. H., and J. B. C. Jackson. 1995. Process from pattern: Tests for selection versus random change in punctuated bryozoan speciation. In *New Approaches to Speciation in the Fossil Record*, edited by D. H. Erwin and R. L. Anstey, 184–207. New York: Columbia University Press.

Cheetham, A. H., J. B. C. Jackson, and L.-A. C. Hayek. 1993. Quantitative genetics of bryozoan phenotypic evolution. I. Rate tests for random change versus selection in differentiation of living species. *Evolution* 47:1526–1538.

Cheetham, A. H., J. B. C. Jackson, and L.-A. C. Hayek. 1994. Quantitative genetics of bryozoan phenotypic evolution. II. Analysis of selection and random change in fossil species using reconstructed genetic parameters. *Evolution* 48:360–375.

Ciampaglio, C. N., M. Kemp, and D. W. McShea. 2001. Detecting changes in morphospace occupation patterns in the fossil record: Characterization and analysis of measures of disparity. *Paleobiology* 27:695–715.

Coyne, J. A. and H. A. Orr. 2004. *Speciation*. Sunderland, MA: Sinauer Associates, Inc.

Davidson, E. H. 2010. *The Regulatory Genome: Gene Regulatory Networks in Development and Evolution*. New York: Academic Press.

Decellea, J., N. Suzukib, F. Mahéa, C. de Vargasa, and F. Nota. 2012. Molecular phylogeny and morphological evolution of the *Acantharia* (Radiolaria). *Protist* 163:435–450. doi:10.1016/j.protis.2011.10.002

Dick, M. H., A. Herrera-Cubilla, and J. B. C. Jackson. 2003. Molecular phylogeny and phylogeography of free-living Bryozoa (Cupuladriidae) from both sides of the Isthmus of Panama. *Molecular Phylogenetics and Evolution* 27:355–371. doi:10.1016/S1055-7903(03)00025-3

Donoghue, P. C. J., and M. J. Benton. 2007. Rocks and clocks: Calibrating the Tree of Life using fossils and molecules. *Trends in Ecology & Evolution* 22:424–431. doi:10.1016/j.tree.2007.05.005

Dornburg, A., J. M. Beaulieu, J. C. Oliver, and T. J. Near. 2011. Integrating fossil preservation biases in the selection of calibrations for molecular divergence time estimation. *Systematic Biology* 60:519–527. doi:10.1093/sysbio/syr019

Drummond, A. J., S. Y. W. Ho, M. J. Phillips, and A. Rambaut. 2006. Relaxed phylogenetics and dating with confidence. *PLoS Biol* 4:e88. doi:10.1371/journal.pbio.0040088

Drummond, A. J., M. A. Suchard, M. A., X. Dong, and A. Rambaut. 2012. Bayesian phylogenetics with BEAUti and the BEAST 1.7. *Molecular Biology and Evolution* 29:1969–973. doi:10.1093/molbev/mss075

Eldredge, N., and S. J. Gould. 1972. Punctuated equilibria: An alternative to phyletic gradualism. In *Models in Paleobiology*, edited by T. J. M. Schopf, 82–115. San Francisco: Freeman Cooper.

Estes, S., and S. J. Arnold. 2007. Resolving the paradox of stasis: Models with stabilizing selection explain evolutionary divergence on all timescales. *American Naturalist* 169:227–244.

Falconer, D. S. 1981. *Introduction to Quantitative Genetics*, 2nd ed. London: Longman Group Ltd.

Frankel, N., D. F. Erezyilmaz, A. P. McGregor, S. Wang, F. Payre, and D. L. Stern. 2011. Morphological evolution caused by many subtle-effect substitutions in regulatory DNA. *Nature* 474:598–603. doi:10.1038/nature10200

Freeland, J. 2006. *Molecular Ecology*. New York: John Wiley & Sons.

Geary, D. H. 1990. Patterns of evolutionary tempo and mode in the radiation of *Melanopsis* (Gastropoda; Melanopsidae). *Paleobiology* 16:492–511.

Geary, D. H., G. Hunt, I. Magyar, and H. Schreiber. 2010. The paradox of gradualism: Phyletic evolution in two lineages of lymnocardiid bivalves (Lake Pannon, central Europe). *Paleobiology* 36:592–614.

Giribet, G, D. L. Distel, M. Pol, W. Sterrer, and W. C. Wheeler. 2000. Triploblastic relationships with emphasis on the acoelomates and the position of Gnathostomulida, Cycliophora, Platheminthes, and Chaetognatha: A combined approach of 18S rDNA sequences and morphology. *Systematic Biology* 49:539–562. doi:10.1080/10635159950127385

Gingerich, P. D. 1983. Rates of evolution: Effects of time and temporal scaling. *Science* 222:159–161. doi:10.1126/science.222.4620.159-a

Gingerich, P. D. 2009. Rates of evolution. *Annual Review of Ecology, Evolution, and Systematics* 40:657–675. doi: 10.1146/annurev.ecolsys.39.110707.173457

Gompel, N., B. Prud'homme, P. Wittkopp, V. A. Kassner, and S. B. Carroll. 2005. Chance caught on the wing: Cis-regulatory evolution and the origin of pigment patterns in *Drosophila*. *Nature* 433: 481–487. doi: 10.1038/nature03235

Gould, S. J., and N. Eldredge. 1993. Punctuated equilibrium comes of age. *Nature* 366:223–227. doi:10.1038/366223a0

Groves, J. R., and S. Reisdorph. 2009. Multivariate morphometry and rates of morphologic evolution within the Pennsylvanian fusulinid *Beedeina* (Ardmore Basin, Oklahoma, USA). *Palaeoworld* 18:120–129. doi:10.1016/j.palwor.2008.12.001

Hageman, S. J. 1994. Microevolutionary implications of clinal variation in the Paleozoic bryozoan *Streblotrypa Lethaia* 27:209–222. doi: 10.1111/j.1502-3931.1994.tb01411.x

Hageman, S. J. 2003. Book Review. *From DNA to Diversity: Molecular Genetics and the Evolution of Animal Design*, by Carroll, Grenier, and Weatherbee (2001). *Journal of Paleontology* 77:598.

Hageman, S. J., M. Bayer, and C. D. Todd. 1999. Partitioning phenotypic variation: Genotypic, environmental, and residual components from bryozoan skeletal morphology. *Journal of Natural History* 33:1713–1735. doi:10.1080/00222939299815

Hageman, S. J., L. L. Needham, and C. D. Todd. 2009. Threshold effects of food concentration on the skeletal morphology of the bryozoan *Electra pilosa* (Linnaeus, 1767). *Lethaia* 42:438–451. doi:10.1111/j.1502-3931.2009.00164.x

Hageman, S. J., P. N. Wyse Jackson, A. R. Abernethy, and M. Steinthorsdottir. 2011. Calendar scale, environmental variation preserved in the skeletal phenotype of a fossil bryozoan (*Rhombopora blakei* n. sp.), from the Mississippian of Ireland. *Journal of Paleontology* 85:853–870.

Hayek, L.-A. C., and E. Bura. 2001. On the ends of the taxon range problem. In *Evolutionary Patterns: Growth, Form, and Tempo in the Fossil Record in Honor of Allan Cheetham*, edited by J. B. C. Jackson, S. Lidgard, and F. K. McKinney, 221–422. Chicago: University of Chicago Press.

Herrera-Cubilla, A., M. H. Dick, J. Sanner, and J. B. C. Jackson. 2006. Neogene Cupuladriidae of tropical America. I: Taxonomy of recent *Cupuladria* from opposite sides of the Isthmus of Panama. *Journal of Paleontology* 80:245–263.

Herrera-Cubilla, A., M. H. Dick, J. Sanner, and J. B. C. Jackson. 2008. Neogene Cupuladriidae of tropical America. II: Taxonomy of recent *Discoporella* from opposite sides of the Isthmus of Panama. *Journal of Paleontology* 82:279–298.

Hoekstra, H. E., and J. A. Coyne. 2007. The locus of evolution: Evo devo and the genetics of adaptation. *Evolution* 61:995–1026. doi: 10.1111/j.1558-5646.2007.00105.x

Hunt, G. 2010. Evolution in fossil lineages: Paleontology and the origin of species. *American Naturalist* 176:S61–S76. doi:10.1086/657057

Hunt, G. 2012. Measuring rates of phenotypic evolution and the inseparability of tempo and mode. *Paleobiology* 2012:351–373.

Hunter, E., and R. N. Hughes. 1994. The influence of temperature, food ration, and genotype on zooid size in *Celleporella hyalina* (L.). In *Biology and Palaeobiology of Bryozoans*, edited by P. J. Hayward, J. S. Ryland, and P. D. Taylor, 83–86, Fredensborg, Denmark: Olsen and Olsen.

Jagadeeshan, S., and A. O'Dea. 2012. Integrating fossils and molecules to study cupuladriid evolution in an emerging Isthmus. *Evolutionary Ecology* 26:337–355. doi:10.1007/s10682-011-9522-6

Jackson, J. B. C., and A. H. Cheetham. 1990. Evolutionary significance of morphospecies: A test with cheilostome Bryozoa. *Science* 248:579–583. doi: 10.1126/science.248.4955.579

Kidwell, S. M., and D. W. Bosence. 1991. Taphonomy and time-averaging of marine shelly faunas. In *Taphonomy: Releasing the data locked in the fossil record*, edited by P. A. Allison and D. E. G. Briggs, 115–209. New York: Plenum.

Kimura, M., 1980. A simple method for estimating evolutionary rate of base substitutions through comparative studies of nucleotide sequences. *Journal of Molecular Evolution* 16:111–120. doi:10.1007/BF01731581

Kowalewski, M., and R. K. Bambach. 2008. The limits of paleontological resolution. In *High-Resolution Approaches in Stratigraphic Paleontology.* Topics in Geobiology, vol. 21, edited by P. J. Harries, 1–48. Dordrecht: Springer Netherlands.

Kumar, S. 2005. Molecular clocks: Four decades of evolution. *Nature Reviews Genetics* 6:654–662. doi:10.1038/nrg1659

Knowlton, N. 1993. Sibling species in the sea. *Annual Review of Ecology and Systematics* 24:189–216. doi:10.1146/annurev.es.24.110193.001201

Lazarus, D. 1986. Tempo and mode of morphologic evolution near the origin of the radiolarian lineage *Pterocanium prismatium*. *Paleobiology* 12:175–189.

Levinton, J. S. 2001. *Genetics, Paleontology, and Macroevolution*, 2nd ed. Cambridge: Cambridge University Press.

Lydeard, C., M. C. Wooten, and A. Meyer. 1995. Molecules, morphology, and area cladograms: A cladistic and biogeographic analysis of *Gambusia* (Teleostei: Poeciliidae). *Systematic Biology* 44:221–236. doi:10.1093/sysbio/44.2.221

Marshall, C. R. 1990. Confidence intervals on stratigraphic ranges. *Paleobiology* 16:1–10.

Marshall, C. R. 1997. Confidence intervals on stratigraphic ranges with nonrandom distributions of fossil horizons. *Paleobiology* 23:165–173.

McPeek, M. A., L. B. Symes, D. M. Zong, and C. L. McPeek. 2010. Species recognition and patterns of population variation in the reproductive structures of a damselfly genus. *Evolution* 65:419–428. doi: 10.1111/j.1558-5646.2010.01138.x

Mishler, B. D. 1994. Cladistic analysis of molecular and morphological data. *American Journal of Physical Anthropology* 94:143–156. doi:10.1002/ajpa.1330940111

Nee, S. 2004. Extinct meets extant: Simple models in paleontology and molecular phylogenetics. *Paleobiology* 30:172–178.

Nei, M., and S. Kumar. 2000. *Molecular Evolution and Phylogenetics*. New York: Oxford University Press.

Omland, K. E. 1997. Correlated rates of molecular and morphological evolution. *Evolution* 51:1381–1393.

Oros, M., T. Scholz, V. Hanzelová, and J. S. Mackiewicz. 2010. Scolex morphology of monozoic cestodes (Caryophyllidea) from the Palaearctic Region: A useful tool for species identification. *Folia Parasitologica* 57:37–46.

Pachut, J. F., and R. L. Anstey. 2009. Inferring evolutionary modes in a fossil lineage (Bryozoa: *Peronopora*) from the Middle and Late Ordovician. *Paleobiology* 35:209–230.

Pagel, M., C. Venditti, and A. Meade. 2006. Large punctuational contribution of speciation to evolutionary divergence at the molecular level. *Science* 314:119–121. doi: 10.1126/science.1129647

Prud'homme, B., N. Gompel, and S. B. Carroll. 2007. Emerging principles of regulatory evolution. *Proceedings of the National Academy of Science* 104:8605–8612. doi:10.1073/pnas.0700488104

Prud'homme, B., N. Gompel, A. Rokas, V. A. Kassner, T. M. Williams, S. D. Yeh, J. R. True, and S. B. Carroll. 2006. Repeated morphological evolution through cis-regulatory changes in a pleiotropic gene. *Nature* 440:1050–1053. doi:10.1038/nature04597

Quental, T. B., and C. R. Marshall. 2010. Diversity dynamics: Molecular phylogenies need the fossil record. *Trends in Ecology and Evolution* 25:434–441. doi: 10.1016/j.tree.2010.05.002

Renaud, S., J. C. Auffray, J. Michaux. 2007. Conserved phenotypic variation

patterns, evolution along lines of least resistance, and departure due to selection in fossil rodents. *Evolution* 60:1701–1717. doi:10.1111/j.0014-3820.2006.tb00514.x

Rebollo, R., B. Horard, B. Hubert, and C. Vieira. 2010. Jumping genes and epigenetics: Towards new species. *Gene* 454:1–7. doi:10.1016/j.gene.2010.01.003

Rieseberg, L. H., and B. K. Blackman. 2010. Speciation genes in plants. *Annals of Botany* 106:439–455. doi:10.1093/aob/mcq126

Ricklefs, R. W. 2006. Time, species, and the generation of trait variance in clades. *Systematic Biology* 55:151–159. doi:10.1080/10635150500431205

Riisgård, H. U., and A. Goldson. 1997. Minimal scaling of the lophophore filter-pump in ectoprocts (Bryozoa) excludes physiological regulation of filtration rate to nutritional needs: Test of hypothesis. *Marine Ecology Progress Series* 156:109–120.

Roopnarine, P. D. 2003. Analysis of rates of morphologic evolution. *Annual Review of Ecology, Evolution, and Systematics* 34:605–632. doi:10.1146/annurev.ecolsys.34.011802.132407

Roopnarine, P. D, G. Byars, and P. Fitzgerald. 1999. Anagenetic evolution, stratophenetic patterns, and random walk models. *Paleobiology* 25:41–57.

Ruse, M. 2000. The theory of punctuated equilibria: Taking apart a scientific controversy. In *Scientific Controversies: Philosophical and Historical Perspectives*, edited by P. Machamer, M. Pera, and A. Baltas, 230–253. New York: Oxford University Press.

Sadler, P. M. 1981. Sediment accumulation rates and the completeness of stratigraphic sections. *Journal of Geology* 89:569–584.

Sadler, P. M. 2004. Quantitative biostratigraphy: Achieving finer resolution in global correlation. *Annual Reviews of Earth and Planetary Science* 32:187–213. doi: 10.1146/annurev.earth.32.101802.120428

Sanderson, M. J. 2002. Estimating absolute rates of molecular evolution and divergence times: A penalized likelihood approach. *Molecular Biology and Evolution* 19:101–109.

Shubin, N. 2008. *Your Inner Fish: A Journey into the 3.5-Billion-Year History of the Human Body*. New York: Pantheon Books.

Stanley, S. M., and X. Yang. 1987. Approximate evolutionary stasis for bivalve morphology over millions of years: A multivariate, multilineage study. *Paleobiology* 13:113–139.

Stone, J. R., and G. A. Wray. 2001. Rapid evolution of cis-regulatory sequences via local point mutations. *Molecular Biology and Evolution* 18:1764–1770.

Theissen, G. 2006. The proper place of hopeful monsters in evolutionary biology. *Theory in Biosciences* 124:349–369. doi:10.1016/j.thbio.2005.11.002

Wahlberg, N., and S. Nylin. 2003. Morphology versus molecules: Resolution of the positions of *Nymphalis*, *Polygonia*, and related genera (Lepidoptera: Nymphalidae). *Cladistics* 19:213–223. doi:10.1111/j.1096-0031.2003.tb00364.x

Wittkopp, P. J., and G. Kalay. 2012. Cis-regulatory elements: Molecular mechanisms and evolutionary processes underlying divergence. *Nature Reviews Genetics* 13:59–69. doi:10.1038/nrg3095

Weiss, R. E., and C. R. Marshall. 1999. The uncertainty in the true end point of a fossil's stratigraphic range when stratigraphic sections are sampled discretely. *Mathematical Geology* 31:435–453. doi: 10.1023/A:1007542725180

Yang, Z. 2006. *Computational Molecular Evolution*. New York: Oxford University Press.

Zeh, D. D., J. A. Zeh, and Y. C. Ishi. 2009. Transposable elements and an epigenetic basis for punctuated equilibria. *BioEssays* 31:715–726. doi: 10.1002/bies.200900026

Zuckerkandl, E., and L. Pauling. 1962. Molecular disease, evolution, and genetic heterogeneity. In *Horizons in Biochemistry*, edited by M. Kasha and B. Pullman, 189–225. New York: Academic Press.

Zuckerkandl, E., and L. Pauling. 1965. Evolutionary divergence and convergence in proteins. In *Evolving Genes and Proteins*, edited by V. Bryson and H. J. Vogel, 97–166. New York: Academic Press.